ELSEVIER

PII: S0266-3538(97)00032-8

Composites Science and Technology **57** (1997) 729–737

0266-3538/97/$17.00

MODE II DELAMINATION TOUGHNESS OF STITCHED GRAPHITE/EPOXY TEXTILE COMPOSITES

Bhavani V. Sankar[a] & Suresh K. Sharma[b]

[a] *Department of Aerospace Engineering, Mechanics and Engineering Science, University of Florida, Gainesville, Florida 32611-6250, USA*

[b] *General Electric Corporate R&D Center, Schenectady, New York 12301, USA*

(Received 18 March 1996; revised 3 December 1996; accepted 8 January 1997)

Abstract

Effects of through-thickness stitching on Mode II delamination toughness (G_{IIc}) of graphite/epoxy uniweave textile laminates have been investigated by performing end-notched flexure tests. Different stitch yarns and stitch densities were considered. The crack propagation in stitched laminates was observed to be gradual and steady, unlike in the unstitched laminates where it was sudden. New methods of evaluating the effective or apparent critical strain-energy release rate for stitched laminates are presented. Stitching results in an excellent improvement in G_{IIc}. The apparent G_{IIc} was 5 to 15 times that of the unstitched laminates, depending on the stitching parameters. There appears to be an optimum stitch density at which the toughness will be a maximum. The critical strain-energy release rate increases with increase in crack length as more and more stitches bridge the delamination. © 1997 Elsevier Science Limited

Keywords: textile composites; toughness; delamination; through-thickness reinforcement

1 INTRODUCTION

Although unidirectional laminated composites have high strength in the fiber direction, they lack through-thickness reinforcement. Hence, they have poor interlaminar fracture toughness and are susceptible to delaminations. One of the ways of reinforcing a laminate in the thickness direction is by through-thickness stitching. The techniques and equipment for stitching textile fabrics are well developed, and therefore can be adapted to advanced fiber preforms with relative ease and economy. In the past, researchers have primarily investigated the effects of stitching on free-edge delaminations and Mode I fracture toughness of unidirectional tape laminates.[1,2] The number of papers on the effects of stitching on the Mode II fracture toughness of textile laminates has been very few. Ogo[3] investigated the effect of through-thickness stitching of plain-weave graphite/epoxy laminates with Kevlar yarn. The study showed a manifold increase in the Mode I critical strain-energy release rate, G_{Ic}, at the expense of a slight fall in in-plane properties. However, his results did not show any significant increase (only 8%) in Mode II fracture toughness as characterized by the critical strain-energy release rate, G_{IIc}. Similarly, although some efforts have been made to model the effect of stitching on Mode I fracture toughness,[4–6] no models have been proposed for the Mode II fracture toughness. Recently, Sohn and Hu[7] found experimentally that adding small amounts of chopped Kevlar fiber between continuous carbon-fiber layers can improve Mode II delamination toughness. Dransfield *et al.*[8] presented a thorough review of the effects of stitching on improving delamination resistance of carbon-fiber-reinforced plastic composites. Jain and Mai[9] have developed micromechanics-based models to predict the behavior of stitched end-notched flexure (ENF) specimens.

It is evident from the above studies that through-thickness stitching significantly improves Mode I fracture toughness in laminates made of graphite unidirectional tapes or plain-weave fabric and epoxy resin. Recently, the authors conducted an experimental program to assess the impact and interlaminar fracture properties of through-thickness stitched textile composites. The results of this program[10,11] showed that significant improvements can be achieved in the impact resistance, impact damage tolerance, Mode I and II delamination toughness properties of stitched uniweave textile laminates. In this paper, we report the results of an experimental study on Mode II delamination toughness and describe two methods to evaluate the effective or apparent critical strain-energy release rate.

A modified lock stitch

Fig. 1. Sketch of modified stitch lock.

2 EXPERIMENTAL

2.1 Material system

The stitched uniweave fabric in this testing program consisted of 24 plies of AS4 unidirectional graphite fibers woven with light E-glass filler tows (2·5% by weight). This preform was then stitched through the thickness by using the modified stitch lock shown in Fig. 1. This type of stitch lock does not crimp the top layers of the preform. Three different bobbin stitch yarns of different linear densities were used as shown in Table 1. The Kevlar yarn used as the needle yarn was of low linear density* (400 denier or 11 160 yd lb^{-1}) so that it could go through the needle ear and also penetrate the fabric easily. The same needle yarn was used in all specimens. The three bobbin stitch yarns will be referred to by their yarn numbers as Kevlar-2790, Glass-1250 and Glass-750, the last being the largest in diameter. We define the stitch density as the number of stitches per square inch (SPSI), and represent this density by the stitching pattern as: (number of stitches per inch) × (spacing between two stitch rows). For example, 8 × 1/4 means a stitch density of 32 SPSI, where the pitch is $3{\cdot}175 \times 10^{-6}$ m (1/8 in) and distance between two adjacent stitch rows is $6{\cdot}35 \times 10^{-3}$ m (1/4 in).

Table 1. Details of stitch yarns

Stitch yarn	Breaking strength in N (lbf)
Kevlar (1600 denier ≃ 2790 yd lb^{-1}) bobbin yarn	347 (78)
Glass (3570 denier ≃ 1250 yd lb^{-1}) bobbin yarn	262 (59)
Glass (5952 denier ≃ 750 yd lb^{-1}) bobbin yarn	436 (98)
Kevlar (400 denier ≃ 11 160 yd lb^{-1}) needle yarn	53 (12)

* The thickness of yarns is specified either by denier or yarn number. Denier is the mass in grams of 9000 metres of the yarn. Yarn number is the length in yards of 1 lb of yarn. The product of denier and yarn number is equal to 4 464 000.

2.2 Processing

Two different stitch densities (16 and 64 SPSI) for each of the three stitch yarns were obtained as shown in Table 2. The top and bottom sides of the preform were covered by one ply each of plain-weave glass fiber cloth to retain the stitches. Unstitched control specimens were also processed. The stitched and unstitched preforms were molded with epoxy 3501-6 by using resin-transfer molding (RTM) following the manufacturer's recommended curing cycle. A sketch of a typical processed plate is shown in Fig. 2. A 0·0635 m × 0·66 m Teflon film was implanted at the midplane along the edge to produce a starter crack. No stitching was done within $12{\cdot}7 \times 10^{-3}$ m of the film. All seven plates were ultrasonically C-scanned to ensure good quality, and also to check for any movement of the Teflon film during the RTM process. ENF specimens were cut from the plates and loaded as shown in Fig. 3. A natural starter crack was obtained by extending the crack by about 2 mm. The specimen was held in a machine vice and a sharp surgical knife was used to extend the crack up to the line at which the vice was gripping the specimen.

2.3 ENF test and data reduction

ENF tests were performed to measure Mode II delamination toughness in stroke control mode following the guidelines given by Carlsson and Pipes.[12] The load and displacement were measured by reading signals from a load cell and a linear variable displacement transformer (LVDT) signal into a Nicolet digital oscilloscope. Attempts were made to observe crack propagation with the help of a

Table 2. Material system[a] for interlaminar fracture toughness tests

Plate no.	Stitch density	Stitch yarn	Yarn no.	Denier	Thickness (10^{-3} m)
24	4 × 1/4 in	Kevlar	2790	1600	3·683
25	8 × 1/8 in	Kevlar	2790	1600	4·191
26	4 × 1/4 in	Glass	1250	3570	3·810
27	8 × 1/8 in	Glass	1250	3570	4·191
28	4 × 1/4 in	Glass	750	5952	4·318
29	8 × 1/8 in	Glass	750	5952	4·445
30	None	—	—	—	3·556

[a]Lay-up: unidirectional (stitching is in 0° fiber direction); no. of plies: 24 (each ply is AS4 uniweave cloth).

magnifying lens ($\times 5$) during the test, but the visual method was not very successful because it was difficult to see the crack tip clearly. Preliminary tests with six specimens each of the unstitched and stitched (Kevlar-2790, $4 \times 1/4$) laminates were conducted by loading and unloading to different increasing peak loads to understand the load/displacement pattern. During these tests, the crack front for the unstitched laminates extended suddenly after reaching a critical load. However, in the stitched laminates the crack propagation was steady and gradual as can be inferred by the load/deflection diagram. A large difference in the propagated crack length was observed between the visual and ultrasonic C-scan measurements, confirming that the visual measurements may not be very accurate. Having observed the crack propagation pattern, the remaining specimens were loaded up to a point where the crack front extended approximately up to the midpoint of the specimen, and then completely unloaded. At least six specimens in each category were tested. A load/displacement (P/δ) curve was plotted for each test. Representative load/displacement curves for unstitched and stitched laminates are shown in Figs 4 and 5. A typical P/δ curve for intermediate stages of crack propagation for a stitched laminate is shown in Fig. 5. For the unstitched laminates, the critical load, P_c, to initiate crack propagation was noted, and by using the compliance, C, from the P/δ curve and other specimen dimensions, the critical strain-energy release rate was calculated from the elastic beam theory formula.[12] However, this method is not applicable for stitched laminates and hence two new methods are suggested for estimating the Mode II delamination toughness of stitched laminates.

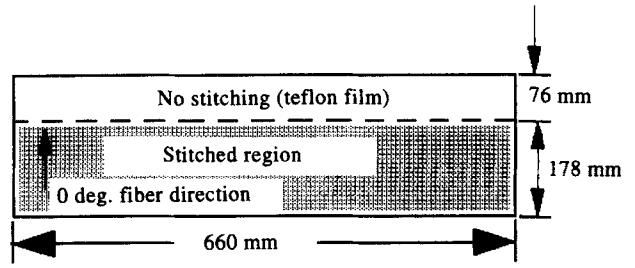

Fig. 2. Schematic representation of a typical resin-transfer-molded stitched graphite/epoxy plate processed to machine ENF specimens.

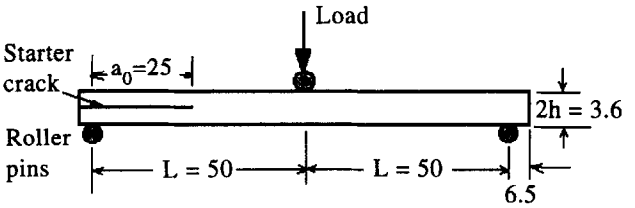

Fig. 3. Schematic diagram of the ENF specimen. All dimensions are in mm.

3 METHODS TO DETERMINE EFFECTIVE MODE II DELAMINATION TOUGHNESS OF STITCHED LAMINATES

3.1 Applicability of beam theory formula for stitched laminates

The existing literature uses the following formula[12] to calculate the critical strain-energy release rate for the

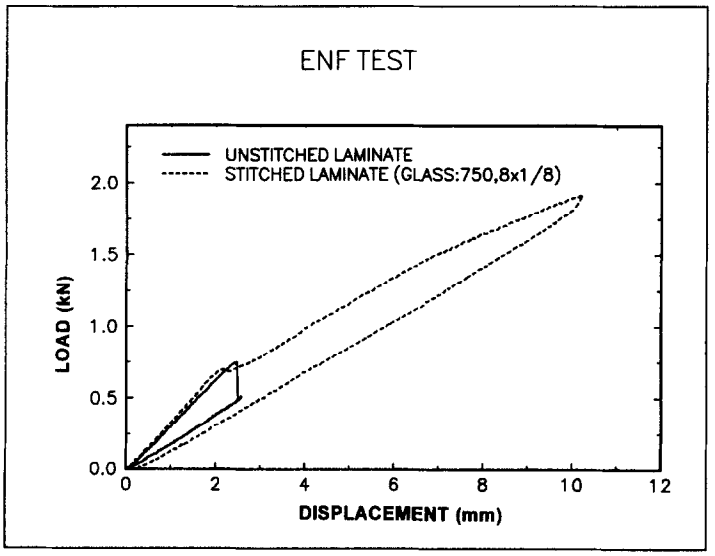

Fig. 4. Representative P/δ curves for unstitched and stitched laminates in the ENF test.

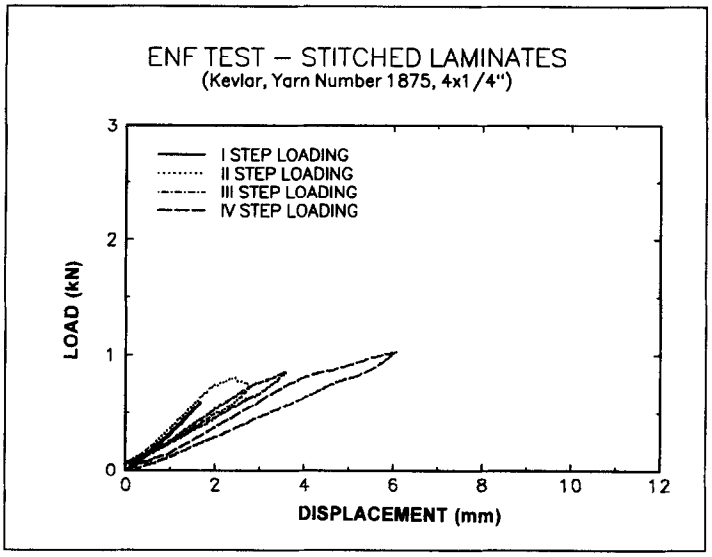

Fig. 5. Typical set of P/δ curves for intermediate steps of crack propagation.

unstitched laminates:

$$G_{IIc} = \frac{9P_c^2Ca^2}{2b(2L^3 + 3a^3)} \quad (1)$$

where b is the width of the specimen, P_c is the critical load at the time of crack propagation and C is the specimen compliance. The average value obtained by this method for the unstitched laminates was 670·72 J m^{-2}.

While the crack propagation in an unstitched laminate was unstable as also indicated by the sudden drop in load on the P/δ curve, the crack propagation in the stitched specimens was observed to be steady. There is no sudden drop in load as the crack starts propagating. The P/δ curves for all the stitched laminates are non-linear after crack propagation begins. That is, the load/deflection curve does not pass through the origin of the graph. This is because the delamination grows continuously and the compliance of the specimen gradually changes as the crack propagates. Therefore, use of the beam theory formula with non-linear P_c and linear C, as suggested by Ogo,[3] will not give a correct estimate of G_{IIc} in case of stitched laminates. The values of crack propagation measured by ultrasonic C-scans were used in computations for the first of the two new methods presented. The first method necessitates the measurement of crack length by C-scan and may be suitable for a first assessment of the Mode II delamination toughness for a through-thickness reinforced composite laminate. The second method proposed uses the compliance of the unloading curve to first calculate the effective new crack length and then uses this information to determine the Mode II delamination toughness. Therefore, this method is considered equivalent to measuring the effective crack length and then using the energy–area approach. This method eliminates the need for a C-scan. The idea of effective crack length has been considered previously by many researchers, most notably by Williams and co-workers.[13,14]

3.2 Area method with ultrasonic C-scan

In this method, the work performed in extending a crack is computed as usual from the load/deflection curve. The crack extension is measured by ultrasonic C-scanning. The average fracture toughness is computed by dividing the work by the crack extension area.

The steps involved in the C-scan method are as follows:

- ensure that the starter crack is at the first stitch line;
- ensure that the crack propagates to at least few stitches during the test and unload completely;
- calculate the work done, ΔW, from P/δ curve (area enclosed by the loading–unloading curves);
- find the area of extended crack surface, ΔA, by using ultrasonic C-scan; and
- compute the fracture toughness as $G_{IIc} = \Delta W/\Delta A$.

3.3 Equivalent area method using compliance of unloading curve

In this method the work performed, ΔW, is computed as in the previous method. An effective crack length of the specimen is computed from the compliance of the specimen. This compliance is obtained as the inverse of the slope of the unloading curve. The effective crack length, a_{eff}, is obtained from eqn (1). Then the crack

propagation length is equal to $a_{\text{eff}} - a_0$, where a_0 is the length of the initial starter crack.

The steps involved in the equivalent area method are as follows:

- calculate EI from the linear compliance, C, of the loading curve;
- calculate the compliance, C', of the unloaded specimen from the unloading curve;
- calculate the effective crack length, a_{eff}, by using C' and the following formulae (see Appendix A for their derivation):
  For $a < L$

$$C' = \frac{(2L^3 + 3a_{\text{eff}}^3)}{96EI} \tag{2}$$

  For $a > L$

$$C' = \frac{8L^3 - 3(2L - a_{\text{eff}})^3}{96EI} \tag{3}$$

- select the appropriate a_{eff} from of the two calculated above;
- calculate the extended crack surface area as $\Delta A = b(a_{\text{eff}} - a_0)$; and
- compute the fracture toughness as $G_{\text{IIc}} = \Delta W/\Delta A$.

4 RESULTS AND DISCUSSION

4.1 Effect of different stitch yarns and stitch densities

The G_{IIc} values were calculated by means of all three methods described above, i.e. the beam theory formula, the area method with ultrasonic C-scan and the equivalent area method using the compliance of the unloading curve. A bar chart of the average values of the data is given in Fig. 6, which shows the comparison of G_{IIc} values obtained from the beam theory formula and the two methods presented above. As expected, the values of G_{IIc} obtained from the beam theory formulation do not show any appreciable increase, indicating that the intrinsic Mode II critical strain-energy release rate of the material remains same. However, the stitching does significantly improve the effective or apparent G_{IIc} as indicated by the values obtained with use of both area methods. The energy required to propagate the crack is apparently more in the presence of stitches. This

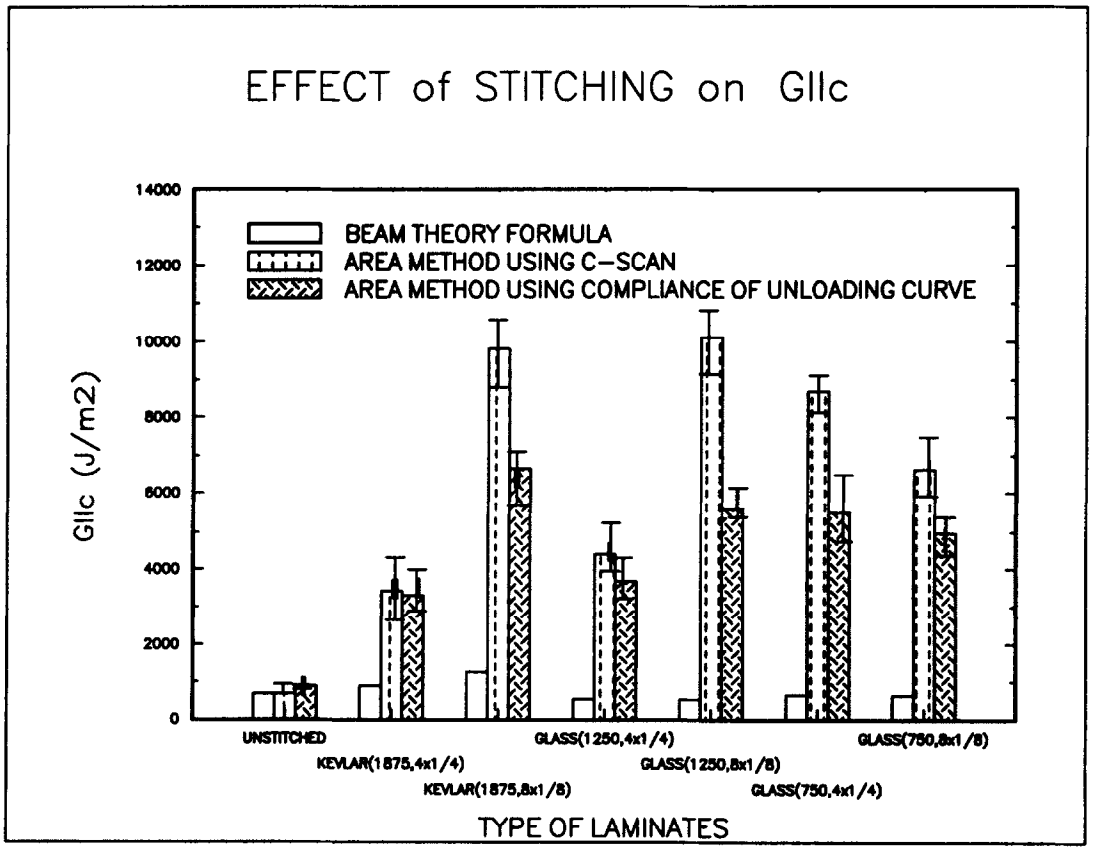

Fig. 6. Effect of stitching on G_{IIc} owing to different stitch yarns and stitch densities. The crack propagated up to the center line ($\Delta a = 0.5 \times L$) approximately.

Table 3. Difference in crack length measurements between ultrasonic C-scanning and the effective crack area method

Specimen no.[11]	Crack length from ultrasonic C-scanning ($\times 10^{-3}$ m)	Crack length from the effective area method (10^{-3} m)
P25S1	41·87	45·79
P25S2	40·94	46·71
P25S3	39·73	47·91
P25S4	38·34	45·18
P25S5	39·13	44·52

increased energy is used in deforming the stitches and also breaking them.

The area method with C-scan seems to provide the upper bound for G_{IIc}, while the equivalent area method using the compliance of the unloading curve gives the lower bound. The increase in apparent G_{IIc} values is very impressive for all the stitch yarns investigated. It is about 5 to 15 times that of the unstitched laminates using the conservative, lower-bound values. It appears that the crack length detected by the C-scanning is smaller than the effective crack propagation length calculated from the compliance of the unloading curve. This may be due to the close contact between the delaminated surfaces. It is also recalled that the propagated crack length could not be accurately resolved visually during the test. An example of differences between the two measurements is presented in Table 3. All the stitch yarns used in this study showed that the apparent G_{IIc} increases with increasing stitch density except for Glass-750, where the change resulting from increased stitch density with this thick bobbin yarn seemed to be slightly smaller, although the values are still higher than those of the unstitched laminates. This suggests that there is perhaps an optimum stitch density for a given yarn.

4.2 Variation of Mode II delamination toughness with crack length

The G_{IIc} values in Fig. 6 were obtained by computing the work done for the entire length of crack propagation in the test and dividing the work by the entire extended area of the crack. Thus it is an average measure of fracture toughness. The effect of crack length on the fracture toughness of stitched laminates (crack resistance curve) can be studied in two different ways. The first is again an average measure. In this method the calculations described in Section 3.3 are performed by assuming that the specimen was unloaded at an intermediate load level, say at the point (δ_1, P_1) (see Fig. 7). Since we did not actually perform the unloading, we assume that the unloading curve was a straight line passing through the origin. This is consistent with the observations made in the

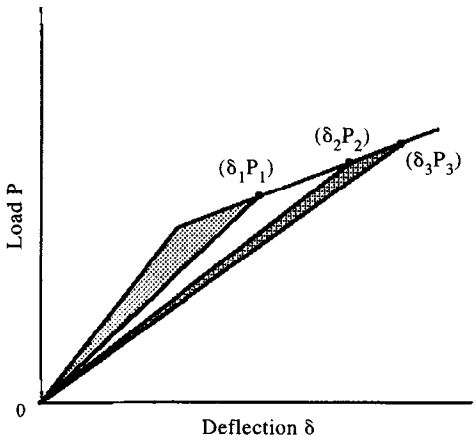

Fig. 7. Schematic representation of the P/δ diagram for the computation of crack resistance.

few loading–unloading tests we performed (see Figs 4 and 5). The equivalent crack length was calculated with eqn (2) or eqn (3). The plot of G_{IIc} as a function of crack length for various specimens is shown in Fig. 8. One can note that the fracture toughness starts from a low value—almost equal to that of the unstitched specimens—and gradually increases with crack length. Further, for the two cases with high stitch density, 64 SPSI Kevlar and 64 SPSI Glass-750, the fracture toughnesses seem to attain a steady-state value at about 18 mm and 22 mm of crack extension, respectively. One can also note a similar tendency in 64 SPSI Glass-1250.

Another measure of crack resistance is an instantaneous G_{IIc} as a function of crack length. In this method we consider two points in the loading curve such that the points are close to each other. In Fig. 7 they are denoted by (δ_2, P_2) and (δ_3, P_3). The area under the P/δ curve between the two points is computed. The crack extension during this incremental

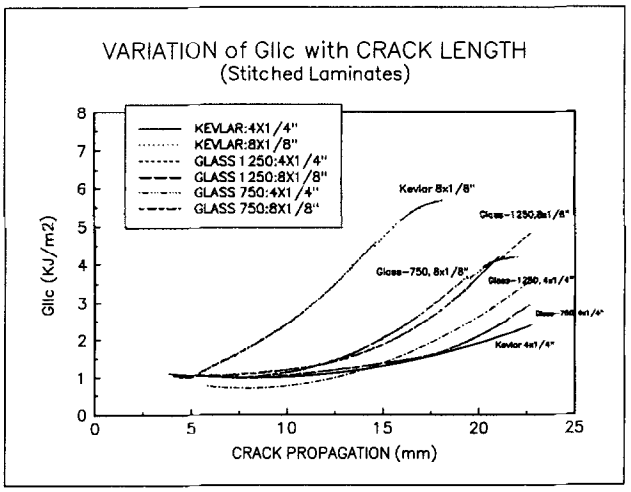

Fig. 8. Variation in G_{IIc} with increase in crack length of stitched laminates.

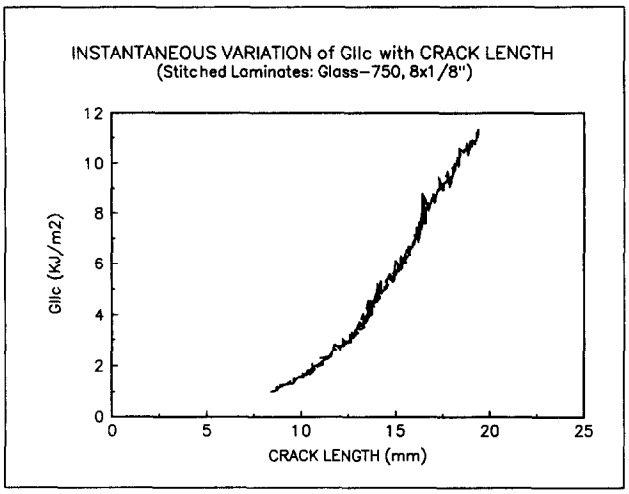

Fig. 9. Variation of instantaneous G_{IIc} as a function of crack length in a stitched laminate.

loading is computed by determining the difference in crack lengths at P_3 and P_2, using eqn (2) or eqn (3). Then the instantaneous G_{IIc} is the incremental work divided by the incremental crack area. The value of instantaneous fracture toughness for 64 SPSI Glass-750 specimens is shown in Fig. 9. One may note that the instantaneous fracture toughness can be very high compared with the average fracture toughness.

The increase in fracture toughness as the crack propagates towards the mid-span of the beam can be attributed to other factors also. For example, there will be tremendous compressive stresses beneath the loading point, and the friction between the delaminated surfaces could artificially increase the apparent fracture toughness. Thus the values of fracture toughness obtained when the crack tip is close to the loading point need to be interpreted carefully.

4.3 Stitch failure mechanism

4.3.1 Measurement of crack length propagation

Since the crack surfaces do not open like in double cantilever beam (DCB) tests, it is very difficult to see the crack tip in ENF specimens. The crack enhancement technique of painting the side edges with white paint did not work satisfactorily for stitched laminates. X-radiography of the crack surface was attempted. X-ray-opaque fluid solutions of zinc iodide, barium chloride and Conray® were tried in varying concentrations. The capillary action does not seem to be adequate to obtain good contrast. Experiments varying the X-ray intensity were also conducted in the facility at the University's Medical Center. Changes in the distance to the specimen, soaking time for capillary action, X-ray exposure times, and different photographic films were all tried without satisfactory results. The primary problem appears to be the inability of the X-ray-opaque dye to penetrate into the extremely narrow crack space, or the relative opening of the crack was insufficient so that the opaque solution was not concentrated enough. Ultrasonic C-scanning did reveal the crack length but this technique also measures less than the effective crack length. Future experimental work may explore a more accurate method. However, cutting the specimens in small incremental steps starting from the undamaged end confirmed that the first stitch line did not break even though the crack as seen from the C-scan had propagated at least up to the center line of the specimen.

4.3.2 Matrix and stitch yarn deformation

The stitch yarn contribution to the increase in Mode II delamination toughness and the associated matrix deformation mechanisms were investigated. It was observed during cutting of the tested specimens that it is not possible to split open any of the cracked specimens even though C-scans showed the crack front to have propagated to as much as half the total specimen length or more. The type of stitches used in this study did not break—or, at best, it is conjectured that perhaps the first one or two stitches may have partially broken. The crack front appears to have traveled around the stitch yarn. Owing to the uniweave architecture of the fabric there was no additional resistance except that of the matrix and the glass fill yarn (2·5%) used in the uniweave cloth during fabric manufacture. This is analogous to stitch yarn 'ploughing' through the matrix. The 'ploughing' represents energy expended in deformation of the matrix. This explains why the fracture toughness increases by the same amount for Kevlar-2790 and Glass-1250 which are closer to each other in diameter, while the Glass-750, being thicker, gives a higher rise in delamination toughness for $4 \times 1/4$ stitch density. The thicker the yarn, the greater was the deformation of the matrix. Also, the delamination toughness increases with increase in stitch density (except for Glass-750), indicating increased matrix deformation. In the case of $8 \times 1/8$ Glass-750, the fracture toughness in fact drops compared with $4 \times 1/4$ Glass-750; this may be a consequence of the excessive density of the thick yarn making the smaller less matrix volume now available easier to 'plough'. This also indicates that there is a possible optimum stitch density for desired fracture toughness and design loading requirements.

A similar effect was observed by Helfet and Harris[15] and Hing and Groves.[16] In both works, the fracture toughness of composites reinforced with short discontinuous fibers was studied. The situation of short fibers enhancing the fracture toughness of the matrix is indeed similar to that in stitched composites, wherein

the stitches play the rôle of discontinuous fibers in the aforementioned studies. In both studies plastic shearing of the fibers contributed to the fracture toughness.

5 CONCLUSIONS

Stitching significantly improves the Mode II delamination toughness of uniweave graphite/epoxy laminates. The increase in apparent G_{IIc} was 5 to 15 times when the crack was allowed to propagate up to about center line of the laminates. As the crack surfaces do not open during the ENF test, and it is difficult to estimate the crack length by any method such as visual, X-radiography or ultrasonic C-scan. The ultrasonic C-scan seems to underestimate the effective crack length. Two new methods to calculate apparent G_{IIc} have been developed: one considers the work done as the area under the P/δ curve and uses the C-scan area of the crack surface; the second method uses the compliance of the unloading curve. The critical strain-energy release rate increases with increase in crack length. This is because not all the energy imparted to the laminate goes directly to the crack front. Part of it is used in deforming the stitches and the surrounding matrix material. The stitched laminate seems to behave more like a structure rather than a material. The stitches did not break during these tests. The stitch yarn seems to plough through the matrix. Therefore, as the crack starts propagating, the ploughing resistance increases resulting in increased Mode II fracture toughness.

ACKNOWLEDGEMENTS

This research was conducted under NASA grant NAG-1-1226 to the University of Florida. The authors thank Mr C. C. Poe Jr and Mr W. C. Jackson of NASA Langley Research Center, Hampton, Virginia, for their support and constant encouragement. The authors are grateful to the reviewer for many helpful comments and suggestions.

REFERENCES

1. Mignery, L. A., Tan, T. M. and Sun, C. T., The use of stitching to suppress delamination in laminated composites. In *ASTM STP 876*. American Society for Testing and Materials, Philadelphia, PA, 1985, pp. 371–385.
2. Dexter, H. B. and Funk, J. G., Impact resistance and interlaminar fracture toughness of through-the thickness reinforced graphite/epoxy. AIAA Paper 86-1020-CP, 1986.
3. Ogo, Y., The effect of stitching on in-plane and interlaminar properties of carbon–epoxy fabric laminates. CCM Report Number 87-17, Center for Composite Materials, University of Delaware, Newark, May 1987, pp. 1–188.
4. Pelstring, R. M. and Madan, R. C., Stitching to improve damage tolerance of composites. In *Proc. 34th Int. SAMPE Symposium*, May 1989. SAMPE, Covina, CA, pp. 1519–1528
5. Chen, V. L., Wu, X. X. and Sun, C. T., Effective interlaminar fracture toughness in stitched laminates. In *Proc. 8th Annual Technical Meeting of the American Society of Composites*, Cleveland, OH, 1993, pp. 453–462.
6. Jain, L. K. and Mai, Y., On the effect of stitching on Mode I delamination toughness of laminated composites. *Compos. Sci. Technol.* 1994, **51**, 331–345.
7. Sohn, M. S. and Hu, X. Z., Mode II delamination toughness of carbon-fibre/epoxy composites with chopped Kevlar fibre reinforcement. *Compos. Sci. Technol.* 1994, **52**, 439–448.
8. Dransfield, K., Baillie, C. and Mai, Y.-W., Improving the delamination resistance of CFRP by stitching. *Compos. Sci. Technol.* 1994, **50**, 305–317.
9. Jain, L. K. and Mai, Y.-W., Analysis of stitched laminated ENF specimens for interlaminar Mode II fracture toughness. *Int. J. Fract.* 1994, **68**, 219–244.
10. Sankar, B. V. and Sharma, S. K., Effects of stitching on the fracture toughness of uniweave textile graphite/epoxy laminates. In *Proc. Mechanics of Textile Composites Conf., NASA CP 3311*, Part 2, eds. C. C. Poe, Jr. and C. E. Harris. National Aeronautics and Space Administration, Washington DC, 1995, pp. 481–507.
11. Sharma, S. K. and Sankar, B. V., Effects of through-the-thickness stitching on impact and interlaminar fracture properties of textile graphite/epoxy laminates. NASA Contractor Report 195042, National Aeronautics and Space Administration, Washington DC, 1995.
12. Cadsson, L. A. and Pipes, R. B., *Experimental Characterization of Advanced Composite Materials*. Prentice-Hall, Englewood Cliffs, NJ, 1987, pp. 157–193.
13. Hashemi, S., Kinloch, A. J. and Williams, J. G., Mechanics and mechanisms of delamination in a poly(ether sulphone)–fiber composite. *Compos. Sci. Technol.* 1990, **37**, 429–462.
14. Wang, Y. and Williams, J. G., Corrections for Mode II fracture toughness specimens of composite materials. *Compos. Sci. Technol.* 1992, **43**, 251–256.
15. Helfet, J. L. and Harris, B., Fracture toughness of composites reinforced with discontinuous fibers. *J. Mater. Sci.* 1972, **7**, 494–498.
16. Hing, P. and Groves, G. W., The strength and fracture toughness of polycrystalline magnesium oxide containing metallic particles and fibers. *J. Mater. Sci.* 1972, **7**, 427–434.
17. Sankar, B. V., A finite element for modeling delaminations in composite beams. *Computers and Structures* 1991, **38**, 329–346.

APPENDIX

Expressions for the compliance of an ENF specimen for the cases $a < L$ and $a > L$ are derived by using a novel procedure. The strain-energy release rate of a delaminated beam is simply the difference between

the strain-energy densities U_L (strain energy/unit length of the beam) behind and ahead of the crack tip per unit width:[17]

$$G_{II} = \frac{1}{b}(U_L^{(1)} + U_L^{(2)} - U_L^{(3)}) \tag{A1}$$

where $U_L^{(1)}$ and $U_L^{(2)}$ are the strain-energy densities in the sublaminates behind the crack tip and $U_L^{(3)}$ is that ahead of the crack tip. When the delamination has not reached the mid-span, i.e. $a < L$, the energy densities can be calculated from the bending moments at the crack tip:

$$U_L^{(1)} = U_L^{(2)} = \frac{1}{2EI}\left(\frac{P}{4}a\right)^2 \tag{A2}$$

where P is the load and EI is the flexural rigidity of each of the delaminated sublaminates. Ahead of the crack tip the energy density is

$$U_L^{(3)} = \frac{1}{2}\frac{[(P/2)a]^2}{8EI} \tag{A3}$$

where $8EI$ is the flexural rigidity of the undelaminated section. Substituting from eqn (A2)eqn (A3) into eqn (A1), the strain-energy release rate, G_{II}, can be obtained as

$$G_{II} = \frac{3}{64}\frac{P^2a^2}{bEI} \tag{A4}$$

By definition, the strain-energy release rate is also equal to the rate of change of the elastic strain energy of the beam with respect to the crack surface area:

$$G_{II} = \frac{1}{b}\frac{\partial U}{\partial a} = \frac{1}{2}\frac{P^2}{b}\frac{\partial C}{\partial a} \tag{A5}$$

where C is the compliance of the beam. Equating G_{II} in eqns (A4) and (A5) we obtain:

$$\frac{\partial C}{\partial a} = \frac{3a^2}{32EI} \tag{A6}$$

eqn (A6) can be integrated with respect to a to obtain an expression for C:

$$C = \frac{a^3}{32EI} + C_0 \tag{A7}$$

where C_0 is the constant of integration. It can be seen that C_0 is the compliance of the beam when $a = 0$, i.e. the compliance of the uncracked simply supported beam, which is equal to $L^3/48EI$. Substituting into eqn (A7) we obtain the compliance of the cracked beam as

$$C = \frac{(3a^3 + 2L^3)}{96EI}, (a < L) \tag{A8}$$

When $a > L$, the energy densities are:

$$U_L^{(1)} = U_L^{(2)} = \frac{1}{2EI}\left[\frac{P}{4}(2L - a)\right]^2 U_L^{(3)}$$

$$= \left(\frac{1}{2}\right)\frac{1}{8EI}\left[\frac{P}{2}(2L - a)\right]^2 \tag{A9}$$

The expression for G_{II} can be obtained by substituting from eqn (A9) into eqn (A1) as

$$G_{II} = \frac{3}{64}\frac{P^2(2L - a)^2}{bEI} \tag{A10}$$

Then an equation similar to eqn (A6) can be derived as:

$$\frac{\partial C}{\partial a} = \frac{3}{32EI}(2L - a)^2 \tag{A11}$$

Integrating with respect to a we obtain

$$C = \frac{-1}{32EI}(2L - a)^3 + C_0 \tag{A12}$$

Now, the constant C_0 can be identified as the compliance when the delamination runs through the entire beam length, i.e. $a = 2L$. This compliance, C_0, is equal to $L^3/12EI$. Substituting in eqn (A12) we obtain an expression for the compliance of the delaminated beam for the case $a > L$:

$$C = \frac{8L^3 - 3(2L - a)^3}{96EI}, \quad (a > L) \tag{A13}$$

When the crack propagates to the center of the beam, $a = L$, the expressions for the compliance in eqns (A8) and (A13) match.